# *The Structure Inventory of the Nuclear Pore Complex*



**Citation:** Schwartz, Thomas U. "The Structure Inventory of the Nuclear Pore Complex." Journal of Molecular Biology 428, 10 (May 2016): 1986–2000 © 2016 Elsevier Ltd

**As Published:** http://dx.doi.org/10.1016/J.JMB.2016.03.015

**Publisher:** Elsevier

**Persistent URL:** http://hdl.handle.net/1721.1/116855

**Version:** Author's final manuscript: final author's manuscript post peer review, without publisher's formatting or copy editing

Published in final edited form as:

*J Mol Biol*. 2016 May 22; 428(10 Pt A): 1986–2000. doi:10.1016/j.jmb.2016.03.015.

# The Structure Inventory of the Nuclear Pore Complex

**Thomas U. Schwartz**

Department of Biology, Massachusetts Institute of Technology, Cambridge, MA, USA

## Abstract

The nuclear pore complex is the principal gateway for molecular exchange between nucleus and cytoplasm across the nuclear envelope. Due to its sheer size of estimated 50–112 MDa and its complex buildup from about 500–1000 individual proteins, it is a difficult object to study for structural biologists. Here I review the extensive ensemble of high-resolution structures of the building blocks of the NPC. Concurrent with the increase in size and complexity, these latest, large structures and assemblies can now be used as the basis for hybrid approaches, primarily in combination with cryo-electron microscopic analysis, generating the first structure-based assembly models of the NPC. Going forward, the structures will be critically important for a detailed analysis of the NPC, including function, evolution, and assembly.

## Graphical Abstract

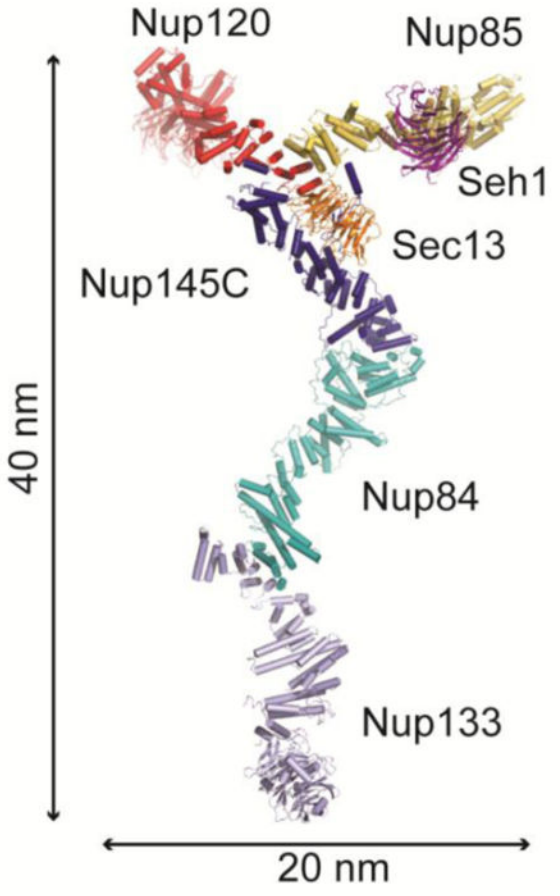


The Y complex of the NPC

## Introduction

One of the hallmarks of eukaryotic life is the compartmentalization of the cell in the form of membrane-enclosed organelles. By establishing a nucleus, eukaryotes spatially separate transcription from translation, which enables the sophisticated gene expression regulation that sets them apart from prokaryotes [1,2]. To cope with the enormous burden of molecular exchange across the nuclear envelope, nuclear pore complexes (NPCs) have evolved to exchange cargo at an enormous speed and with high selectivity. It is estimated that an individual NPC in a human cell can transport up to 80 MDa of material within 1 second [3]. How the NPC is built to perform this task is a central question of cell biology.

NPCs are remarkably complicated and elaborate protein assemblies. Analyzing the protein composition of NPCs from various eukaryotic origin reveals that they all share a set of ~30 nucleoporins (Nups) [4–9]. By various electron microscopic techniques an eightfold rotational symmetry of the NPC is observed, therefore it is assumed that most nucleoporins occur in multiples of eight within the NPC [10–13]. NPCs are positioned in circular

openings that perforate the nuclear envelope, at sites where inner and outer nuclear membrane are fused. Structures of the assembled NPC have been visualized by various EM techniques, with the best resolved density maps obtained using cryo electron tomography (cryo-ET) with human and frog specimen [14,15]. In these maps the principal dimensions and the organization into distinct subassemblies are observable (Figure 1). The donut-shaped NPC is split into three ring moieties, each displaying a lattice-like arrangement. The three rings are termed cytoplasmic ring, inner ring, and nucleoplasmic ring, respectively. The connections between the three rings are less well delineated and appear as rather loose. The three rings are sandwiched between cytoplasmic extensions and a massive nuclear structure called basket. These more peripheral structures are visible in several EM applications [16,17], but they are currently left out from cryo-ET studies of the NPC for technical reasons. A majority of the structural elements of the NPC have been elucidated primarily using X-ray crystallography, mainly over the past decade. This inventory now constitutes an essential component for generating detailed composite structures of the NPC. The level of detail is dictated by the 2–3 nm resolution attained with cryo-ET analysis [14,15,18], which is sufficient to place protein domains in a growing number of NPC subassemblies.

## The assembly from subcomplexes

The NPC is a remarkably modular structure. While the eightfold rotational symmetry was recognized early on in the microscopic analysis of the NPC [19] further degrees of modularity were successively discovered over time. The protein inventory of the NPC has been studied for a very diverse set of eukaryotes, including trypanosomes, fungi, plants, animals and humans [4–9]. In all cases about 30 different nucleoporins were found (Figure 2). Nup names are historically based on their molecular weight. Since the homology between many nucleoporins was not appreciated early on, it lead to the unfortunately convoluted Nup nomenclature of today. However, it is now evident that a set of about 20 nucleoporins appears to be universally conserved among all eukaryotes [8,20,21]. The other ~10 Nups are more divergent and are likely to define species-specific differences. Throughout this review I will use separate abbreviations for *S. cerevisiae* (sc) and *H. sapiens* (hs) as guides through the muddled nomenclature. With mass estimates for the entire NPC ranging from ~50 to ~112 MDa [22–24] it is obvious that this can only be accounted for assuming multiple copies of each Nup. All published stoichiometric measurements are based on the assumption that the eightfold rotational symmetry is maintained on the protein level, i.e., that nucleoporins occur in multiples of eight copies [5,25]. Nucleoporins are organized in a small set of subcomplexes [26], which are primarily defined by the stability of protein interactions. Many of these subcomplexes can be isolated by pull-down experiments [24,27–30]. The stability of them varies from species to species, but that they are principally conserved is generally accepted. The thermophilic fungus *Chaetomium thermophilum* (ct), and its closely related family members, are valuable model organisms since they often provide subcomplexes of higher stability for biochemical and structural analysis [9,31–34].

The largest subcomplex of the NPC is the Y complex, which forms a Y-shaped structure, hence its name [35]. In its simplest from the Y complex has six members, scNup84 (hsNup107), scNup85 (hsNup85), scNup120 (hsNup160), scNup133 (hsNup133), scNup145C (hsNup96), and scSec13 (hsSec13) (Fig. 3a) [33]. Depending on the species, it

can have up to four additional proteins, Nup37, Nup43 ELYS or ELY5, and Seh1 [6,28,36,37]. The Y complex is one of the principal scaffold elements of the NPC that shares intriguing similarities with vesicle coats [38–40]. The Y complex is now considered to be the main component of the nuclear and cytoplasmic rings [14,18,41,42]. The second major scaffold unit is the inner ring complex (IRC), comprising scNup53/59 (hsNup35), scNic96 (hsNup93), scNup188 (hsNup188) or scNup192 (hsNup205), and scNup157/170 (hsNup155) [43]. The trimeric scNsp1 (hsNup62)-scNup57 (hsNup54)-scNup49 (hsNup58) complex is anchored to the IRC via scNic96 (hsNup93) [32,44–46]. Sandwiching the central three-ring stack are cytoplasmic and nucleoplasmic elements. A second pool of scNsp1 (hsNup62) forms a complex together with scNup82(hsNup88) and scNup159 (hsNup214) [47,48], located on the cytoplasmic side. This complex further recruits scDyn2 [49], as well as scNup116 or scNup100 or scNup145N(hsNup98) [50]. HsNup358 is another major cytoplasmic Nup, but missing in yeast.

On the nucleoplasmic side, several proteins, scNup1, scNup2(hsNup50), scNup60, hsNup153 and scMlp1/2(hsTpr) are thought to build up the nuclear basket.

Finally, the NPC assembly is anchored in the pore membrane via a set of transmembrane proteins, scNdc1(hsNdc1), scPom33, scPom34, scPom152, hsPom121 and hsNup210. Below, I take an inventory of the protein structures that make up the NPC and highlight general principles, differences between organisms, and discuss open questions.

## Components of the nuclear ring and the cytoplasmic ring

The notion that the nucleoplasmic and cytoplasmic rings may be predominately built from Y complex units was originally based on immunogold labeling experiments and computational modeling [5,24]. Even though the resolution of these studies was limited, they indicated a tendency for the Y complex components to be more peripheral than the components that are now considered to be the members of the IRC. In addition, Lutzmann et al. showed that the seven Y complex components from *S. cerevisiae* could be recombinantly expressed and reconstituted into a stable assembly of distinct shape, indicating that a high-resolution structural analysis may be feasible [35].

Closely following the technological developments in recombinant protein production, particularly of assemblies, the Y complex has been crystallized in pieces, increasing in size and complexity over the years. Structure prediction tools indicated early on that the majority of the complex would likely be built from mainly two simple elements, stacks of α-helical repeats and β-propeller structures [26,38,51]. Structural comparison with other cellular systems and the understanding that Sec13 is part of the NPC and COPII vesicle coats led to the provocative hypothesis that vesicle coats and the NPC are evolutionarily linked [38,39,52].

Experimental analysis partially confirmed, and partially discredited the computational structure predictions (Figure 3). Sec13, Seh1, Nup37, and Nup43 are indeed all βpropeller proteins [40,53–55]. In addition, scNup120 (hsNup160), Nup133, and hsELYS have N-terminal β-propeller domains, as predicted, each followed by a large, α-helical region

[51,54,56,57]. But this highly simplistic categorization into β-propellers and αhelical repeats glosses over many, structurally highly significant findings.

First, Sec13 and Seh1 fold into unusual six-bladed, open β-propellers, which are closed by a seventh blade provided *in trans* by their respective binding partners. Interestingly, both, Sec13 and Seh1, can be found in complex with multiple proteins. Besides scNup145C (hsNup96) in the NPC, Sec13 can also bind Sec31 and Sec16 in the COPII vesicle coating system [53,58]. These interactions are mutually exclusive. Sec13 and Seh1 are furthermore found as a member of the SEACAT/GATOR2 amino-acid sensing arm of the TOR/mTOR pathway presumably anchored via an insertion-blade as well [59,60].

Second, with regard to the helical domains in scNup84 (hsNup107), Nup85, scNup120 (hsNup160), Nup133, and scNup145C (hsNup96), their three-dimensional structures fall into three distinct categories (Fig. 3d–f). They all form elongated structures, but their helical arrangements are quite distinct [22,57]. We previously categorized the helical domains of scNup84(hsNup107), Nup85 and scNup145C(hsNup96) into one group, which we termed the ancestral coatomer element 1 (ACE1) (Fig. 3d), because it is specifically related to Sec31 and Sec16 in the COPII vesicle system [40,58]. Characteristic for the ACE1 element is a distinct fold-back architecture that involves a core set of ~28 α-helices, generating three subdomains. The first three helices of the ACE1 pair with helices α13–19 to form the trunk, helices α5–11 the crown, and α21–28 the tail [22]. This fold is clearly distinct from the large class of so-called α-solenoid proteins, which are built from continuous stacks of two- or three-helix elements [61]. ACE1 proteins cannot be superimposed on α-solenoid proteins in a meaningful way (Figure 3) and homology modeling programs such as HHpred [62] also distinguish between these folds unambiguously. This structural similarity provides specific, experimental evidence that the NPC and vesicle coating systems have architectural similarities that point to a likely common ancestor dating back to the early eukaryotic evolution.

ScNup120(hsNup160) forms a unique L-shaped molecule, with little overall similarity to any other protein (Fig. 3e) [54,56,63,64]. The N-terminal β-propeller is fully integrated into an ~80 kDa N-terminal domain (NTD) which also contains ~15 additional α-helices. There is no regularity within this helical arrangement. The topology of the scNup120(hsNup160)-NTD, with its interwoven secondary structure elements, suggests that it is rather inflexible. The C-terminal domain (CTD), however, is different. It emanates from the NTD at a 90° angle and is largely built from 7 helical pairs that stack on top of one another similar to HEAT and TPR-repeat proteins. In contrast to the NTD, the CTD allows for significant bending flexibility.

In contrast to scNup120(hsNup160), Nup133 has a flexibly connected N-terminal βpropeller and C-terminal α-helical domain [51,65]. The Nup133-CTD has 28 α-helices and is elongated (Fig. 3f) [57]. It can be split into 4 separate subdomains, which are flexibly connected.

Taken together, the differences in the helical topologies of the Y complex constituents are important in order to understand the possible flexibilities of the assembled Y complex.

Within the past two years, three labs have determined the structure of the assembled Y complex independently, each using a different strategy. Stuwe et al. solved the 7.4 Å crystal structure of a heterohexameric sc(Nup145C-Nup120-Nup85-Nup84-Sec13-Seh1) assembly using a synthetic antibody as a crystallization-chaperone (Fig. 3b) [66]. Kelley et al. solved the 4.1 Å crystal structure of a heterotetrameric Nup120-Nup145C-Nup85-Sec13 assembly from *M. thermophila* (mt) and combined it with previously solved crystal structures to generate a composite structure of the Y complex (Fig. 3a) [33]. Finally, von Appen et al. used a ~2 nm cryo-ET map to build a backbone model of a nonameric human Y complex based on existing crystal structures and homology modeling (Fig. 3c) [14]. All these approaches have their individual strengths and limitations. The heterohexameric yeast structure by Stuwe et al. (Fig. 3b) is the largest continuous Y fragment, but the limited resolution does not allow for complete sequence assignment, and the synthetic antibody may influence the conformation. The heterotetrameric complex by Kelley et al. (Fig. 3a) provides the details of the intricate interaction between the three arms of the Y, but it must be combined with other fragments, from other species, to generate a composite structure. The nonameric human Y structure benefits from using cryo-ET data to being perhaps the closest match to the *in vivo* situation, however, the resolution is rather modest and the model incomplete at the junction of the three arms of the Y structure (Fig. 3c). Taken together, though, these three structures are highly complementary and in combination provide a fairly complete picture of the Y complex. The overall dimensions of the assembly are about 40 nm by 20 nm by 8 nm, reflective of the highly branched shape. When superposed, the three structures are not identical, but differ by the relative position of the three arms. These differences can largely be explained by the expected flexibility of the Y complex and are reflected in observations made in numerous experiments, including EM and crystallographic analyses, modeling, as well as limited proteolysis [14,18,54,66,67].

The purpose of the flexibility in the context of the NPC is not yet understood. The Beck group proposed a model for the CR and NR segments of the NPC, in which eight copies of the Y complex form a circular head-to-tail arrangement [14,18]. Two such eight-membered rings arrange in a slightly offset manner to generate the so-called ‘reticulate two-ring model’. This NPC model requires some flexibility of the Y complex such that it can adopt the two different conformations of the two rings. The observed flexibility of isolated Y complexes is, however, much more pronounced than required for docking into the cryo-ET map [14]. Therefore, one can speculate about several possibilities that may explain the existence of the observed Y complex flexibility. First, averaging procedures in cryo-ET may filter out certain, less populated conformational states of the Y complex; such states may conceivably be more distorted. Second, the assembly pathway of the NPC may require more extreme contortions of the Y complex. Building the 3D structure of the NPC in a confined space, from many subcomplexes, is a complicated puzzle that is difficult to imagine being carried out with rigid protein assemblies. Further, it is unclear if the transport of certain molecules or other factors may require NPC conformational flexibility. Last but not least, the NPC composition may not be monolithic, but possibly the Y complex may need to adapt to different structural contexts, within different NPCs within a cell, or between different cell types.

## Components of the inner ring complex

The IRC of the NPC consists of scNup53/59 (hsNup35), scNic96 (hsNup93), scNup157/170 (hsNup155), Nup188 and scNup192 (hsNup205) [9,31]. The trimeric sc(Nsp1-Nup57-Nup49) hs(Nup62-Nup58-Nup54) FG-Nup complex is anchored to the IRC via scNic96 (hsNup93) [32,45]. The scNup53/59 and scNup157/170 pairs result from the whole genome duplication that occurred about 100 million years ago in yeast evolution, and are therefore specific to *S. cerevisiae* and very close relatives [68]. Other organisms typically have only one paralog of each protein.

The structural characterization of the IRC lags behind the analysis of the Y complex (Fig. 4). scNup53 (hsNup35) is a largely unstructured protein, except for a central 12 kDa dimerization domain (Fig. 4a) [69]. scNic96 (hsNp93) has isolated N-terminal helices, but is otherwise structured around a 65 kDa ACE1 domain (Fig. 4b) [44,70], as described above for the Y complex members Nup84, Nup85, and Nup145C (Fig. 3d). scNup157/170 is completely structurally characterized, and consists of an N-terminal β-propeller loosely integrated with a C-terminal stacked, α-helical domain (Fig. 4c.) [57,71]. It is interesting to note that scNup157/170 (hsNup155) has a recognizable structural homolog in the Y complex as well, namely Nup133 [57]. The helical domains superpose reasonably well, but the N-terminal β-propeller appears to be more flexibly attached in Nup133 [57,71]. These structural similarities between components of the Y complex and the IRC suggest divergent evolution from an ancestral NPC in early eukaryotic evolution, which likely consisted of fewer nucleoporins than all the extant versions of the NPC [38,40,72].

Finally, Nup188 and scNup192 (hsNup205) are the largest universally conserved Nups and their structures are related. Both proteins form superhelical arrangements with considerable flexibility. The predominant shape of the isolated proteins is that of a question mark, as determined by negative stain EM analysis [73,74]. However, other states can also be found in 2D classifications. An N-terminal 110–130 kDa region has been crystallized from mtNup188, scNup192, and ctNup192 [74–76]. In Nup188, the fragment is a circular arrangement of 52 α-helices with an integrated SH3-like domain. In Nup192, the ends of this domain, in contrast, do not meet but arrange to form a lock washer. While the middle, ~40 kDa region of Nup188 and Nup192 is not known experimentally, it can be modeled with high confidence. Together with the crystal structure of the 40 kDa C-terminal domain the full-length structure can be composed reasonably well (Fig. 4d) [74]. The superhelical structures of Nup188 and Nup192 are reminiscent of nuclear transport factors, such as importin-α and importin-β[77–80]. This raised the question of a potential functional relationship. Indeed, mtNup188 and mtNup192 have been shown to have FG-binding activity and they can be transported through the NPC by facilitated diffusion [74] Furthermore, ctNup53 binds ctNup192 involving the same residues with which it also binds importin-α, another indication of relatedness [76]. While the structure inventory of the IRC is largely completed, the assembly is still, compared to the cytoplasmic ring, poorly understood. Binary interactions are well characterized. scNic96(hsNup93) binds Nup188 and scNup192 (hsNup205) in a mutually exclusive manner [32,81]. scNup53 binds scNup192, but not scNup188. And Nup53 also binds Nup157 as well as Nic96 directly. Taken together, a tetrameric ct(Nup53-Nic96-Nup157-Nup192) complex can be assembled

*in vitro*, but it does not seem to adopt a defined three-dimensional structure [31,32]. Consistent with a rather flexible assembly, the interactions sites between the IRC often comprise just short sequence elements, as shown for Nup53 and Nic96. Fitting to this concept of a 'string-puppet-like' assembly of the IRC is that the trimeric Nsp1 complex is primarily anchored to Nic96 only through an extended peptide interaction (Fig. 4e) [32]. The C-terminal, helical portions of Nsp1, Nup57, and Nup49 assemble in a 1:1:1 stoichiometry and together form an unusual tripartite trimeric coiled-coil, which folds back to form a 'number 4' shaped structure (Fig. 4e). This trimeric assembly then binds a 40-residue peptide of Nic96, which seems to serve as a flexible anchor to the IRC. The trimeric assembly is likely conserved in all eukaryotes, as exemplified by the very similar trimeric Nup62-58-54 complex structure from *X. laevis* (Fig. 4f) [45].

Another curious element of the IRC is scNup145N (hsNup98), which is autocatalytically generated from its precursor scNup145 (hsNup98–96), together with scNup145C (hsNup96) [82]. ScNup145C (hsNup96), as mentioned above, is a core member of the Y complex, where it connects the long stalk to the hub. Nup145N has multiple binding partners, including Nup145C, as well as Nup157 and Nup192 in the IRC [31,32], and also Nup82 on the cytoplasmic side [50] (see below).

## Components of the cytoplasmic side

Several nucleoporins are exclusively localized to the cytoplasmic side of the NPC and build the substructure commonly referred to as the cytoplasmic filaments (CFs). In comparison to the central three ring architecture of the NPC, the CFs are very different between species and need to be discussed separately.

In yeast, CFs comprise Nup82, Nup159, Gle1, Gle2, Dyn2, and Nup42 (Fig. 2). Nup82, Nup159, together with a pool of Nsp1 that is separate from the central Nsp1-Nup57-Nup49 complex, form a trimeric 1:1:1 complex at the base of the filaments [48,83]. The three proteins are likely held together by an interaction between their C-terminal coiled-coil regions. Dyn2 is recruited to this complex via Nup159 [49,84]. In addition, the N-terminal β-propeller domain of Nup82 interacts with Nup159 through a second interface (Fig. 5a) [85]. The Nup82 β-propeller further recruits Nup145N, Nup100 or Nup116 via their autoproteolytic domains, in a mutually exclusive manner [50,85]. This way, Nup116 anchors the mRNA export factor Gle2 through a GLEBS motif within its FG-rich, disordered N terminus [86].

At the N-terminal end of Nup159, separated by a long FG-rich middle segment, its βpropeller domain interacts with the RNA helicase Dbp5, which is regulated by its binding partner Gle1 (Fig. 5b) [87]. Finally, Gle1 recruits the FG-Nup Nup42 to complete the cytoplasmic filaments [88]. Anchoring of the cytoplasmic filaments to the NPC core is not entirely clear, but Nup100, Nup116, or Nup145N may play an important role through interaction with Nup192 [31,32]. Importantly, this interaction requires the central, disordered protein segment of Nup145N (or Nup100 or Nup116). While Nup145N can also bind Nup145C of the CR, this interaction is mutually exclusive with Nup82 binding. Therefore, Nup145C cannot serve as an anchoring point for the cytoplasmic filaments [50].

The human CFs are more elaborate than their counterparts in yeast. This is primarily due to the presence of the vertebrate-specific Nup358, a massive, multidomain protein [89,90]. Nup358 contains an N-terminal ~80 kDa stacked α-helical domain followed by eight independent Ran-binding elements. Four of these elements are either Ran-GTP binding domains (RanBDs) [91] or Ran-GDP binding zinc finger modules [92,93]. RanBD has been shown to be critically important for protein export, specifically the disassembly of cargo-NTR-RanGTP complexes [94–97]. The exact role of the Ran-GDP binding zinc fingers is still unclear, but one reasonable hypothesis is that they help in creating a 'Ran sink' at the NPC periphery. Such a function may be unnecessary in yeast, where the cell volume is much smaller (40–80fl for yeast vs. 500–4000fl for human cells) [98] and protein diffusion may suffice to replenish the Ran pool at the NPC. An E3 ligase domain, critical for RanGAP recruitment to the NPC [99–101], and a cyclophilin domain [102,103] complete Nup358.

The CF elements described for yeast are conserved in human as well. Although the human Nups are not tested as extensively as the fungal Nups, phylogenetic analysis suggests that the binary interactions between orthologs should be conserved across species. Thus, CFs share conserved features across all species, but vertebrates in particular have acquired additional functions.

One major function of the cytoplasmic filaments is the regulation of mRNA export, a process which is covered in several recent reviews [104–106].

## Components of the nuclear basket

The nuclear basket of the NPC is structurally poorly understood. In yeast, it contains Nup1, Nup2, Nup60, Mlp1 and Mlp2. Nup1, Nup2 and Nup60 all harbor large FG-extensions combined with rather small, folded regions (Fig. 2). Nup1 and Nup60 have recently been shown to induce membrane curvature, mediated by an N-terminal amphipathic helix, followed by a short helical regions that infers NPC binding [107]. How these helical regions specifically connect to the NPC is not yet known. Similarly, Nup2 has been localized to the nucleoplasmic side, but the molecular details of its NPC integration are unknown. The bulk of the nuclear basket is likely built of Mlp1 and Mlp2, two related ~210 kDa proteins primarily composed of predicted coiled-coil regions [108]. Again, the direct interaction with the NPC core, as well as any detail on forming the distal ring through which the eight nucleoplasmic filaments are co-joined is not clear yet [109]. In humans, the nuclear basket contains, at least, hsTpr (scMlp1/2 ortholog), hsNup50 (scNup2 ortholog) and Nup153. The latter contains Ran-GDP binding zinc finger modules [92,93] closely related to those found in Nup358 on the CFs.

The lack of structural knowledge of the basket is unfortunate, but can likely be contributed to the difficulty of working with large proteins such as hsTpr (scMlp1/2). Since the nuclear basket is involved in various important processes, such as mRNA export and DNA repair [110], the field would benefit immensely from a better structural understanding.

## Membrane nucleoporins

Membrane anchorage of the NPC is another element of the NPC whose structural analysis is yet underdeveloped. Two types of direct membrane interaction are observed among nucleoporins, namely through amphipathic or through transmembrane helices. Amphipathic helices can partially insert into the membrane. This way, they can either induce or sense positive membrane curvature[111–113]. The N-terminal β-propellers of scNup120, hsNup133 and xlNup155 have all been shown to contain curvature-sensing amphipathic lipid packing sensor (ALPS) motifs and therefore are candidates for membrane binding [65,114]. For hsNup133 and xlNup155 this has been experimentally confirmed [14,114,115]. ScNup53, scNup1, and scNup60, on the other hand, appear to induce membrane curvature upon binding via amphipathic helices [107,116]. In contrast, Ndc1, scPom33, scPom34, and scPom152 are all Nups with trans-membrane helices. While Ndc1 is the only universally conserved transmembrane-Nup, even this protein is not essential [117], except in yeast, where it has a second, critical function in the spindle pole body [118,119]. Therefore, it is possible that, in the end, the amphipathic helices are more important for NPC anchorage to the pore membrane than the transmembrane helices are. To say so conclusively, structural studies of the relevant proteins and subcomplexes, including the membrane, will be necessary.

## Integrative approaches to determine the structure of the assembled NPC

The combined efforts, from several labs over the past decade, to determine crystal structures of nucleoporins have generated an invaluable set of building blocks that can now be used for integrative approaches to determine the assembled NPC structure. The assembled NPC is currently best studied by cryo-ET. This approach generates structures of 2–4 nm resolution, using a number of clever experimental tricks to improve the intrinsically high signal-to-noise ratio of the recorded images [14,15,120]. While docking of crystal structures into EM maps is highly accurate below ~10 Å resolution, when secondary structure elements start to become visible, reasonable assumptions can already be made at the current stage. This is particularly true for the Y complex, due to its large and relatively distinct shape, albeit with the caveat of being relatively flexible. The Beck group was the first to seriously attempt to position multiple copies of the Y complex into the cryo-ET map of a human NPC [18]. The proposed model has eight Y-complexes arranged in so-called ‘head-to-tail’ rings, with the ‘head’ defined as the Nup120 arm of the Y complex, and the ‘tail’ defined as Nup133, positioned at the end of the long stalk. These rings are positioned symmetrically, both on the nucleoplasmic and the cytoplasmic side of the NPC [14]. Density analysis further suggests that CR and NR both contain two rings each, for a total of 32 copies of the Y complex per human NPC [14,18]. Positioning the components of the IRC is much more difficult and still tentative, primarily due to the absence of crystal structures of large assemblies. Another problem is that the current cryo-ET resolution does not allow for a proper distinction between various scaffold nups, which look rather indistinguishable at this level of detail. However, there is no doubt that the two approaches are converging and that the existing resolution gap will narrow over time. One important technique might be especially useful going forward, namely single particle cryo electron microscopy (cryo-EM). Using this method, one should be able to obtain larger subassemblies and visualize them at near atomic

resolution [121,122]. The most prominent bottleneck going forward are the ill-defined contact sites between neighboring subcomplexes, which appear to be only weakly bound to one another. Establishing those contact sites with high confidence will undoubtedly further refine current models of the assembled NPC.

## Differences between species

While a majority of nucleoporins is conserved between all eukaryotes, it is becoming obvious that the NPC structures of various species have substantial differences. Those differences are especially pronounced when examining the nucleoplasmic and cytoplasmic extensions of the NPC by scanning electron microscopy [13,16,123], but they also include the three main scaffolding rings. Size estimates for the metazoan NPC and its yeast counterpart differ dramatically (~112 MDa vs. ~50 MDa) [22–24]. Unfortunately, an *in situ* tomographic reconstruction of the yeast NPC does not yet exist, which would provide the best data to differentiate possible gross differences between the species. Without that data, one is largely left with speculations. Since the core scaffold elements are mostly conserved (Fig. 2), a difference in mass by more than a factor of 2 would be most easily explained by differences in Nup copy numbers. For instance, the cytoplasmic and nucleoplasmic 8-membered Y complex double rings, observed in the human NPC, may indeed only be single rings in yeast. Knockdown of the cytoplasmic and metazoan-specific Nup358 reduces the CR to a single ring, without a catastrophic effect for the NPC integrity as a whole [14]. This indicates that the difference between a single- and a double-Y ring may be smaller than anticipated. Another important aspect to consider is that the Y complex itself, for example, is about 50% larger in mass in human versus in thermophilic fungi. Such differences may well exist in other subcomplexes, too. Another ill-defined aspect of the NPC architecture is the potential role that nuclear transport receptors (NTRs) may play in it. NTRs are well known for their role in facilitating cargo transport through the NPC [77,124,125]. However, the evolutionary relationship between NTRs and certain scaffold nups [74–76] indicates that a strict separation of function may be an oversimplification. Together with the dynamic nature of the NPC, i.e., specific Nups with rather short dwell times [126], it may take a considerable effort to establish the molecular differences between NPCs from diverse eukaryotes.

## Outlook

Much progress has been made toward the complete structural characterization of the NPC, one of the largest macromolecular complexes in the cell. We are witnessing the integration of experimental data from different sources providing first models of the assembled NPC. Improvements on experimental and computational techniques will further refine existing NPC models over the next decade. A particularly important role will likely be played by cryo-EM methods, which may substitute crystallographic analysis going forward. Particularly the analysis of subassemblies should profit from the ongoing revolution in EM technology [127,128]. The next big challenge is to arrive at a complete molecular description of the NPC, ideally by positioning all individual Nups within the NPC. Due to the dynamic nature of the NPC this will not be a simple endeavor. Progress will depend on finding tailored solutions for the specific challenges of the system. A molecular description

of the NPC should provide a test bed for dissecting the many diverse functions that NPCs perform, which I have mentioned in this review only in passing. Discovering the specific differences between the NPC architecture of diverse species may be particularly insightful to trace the evolution of this ancient eukaryotic invention and to unravel adaptations to diverse life styles.

## Acknowledgments

I thank all past and present members of my lab for their efforts and insights.

I would like to apologize to all colleagues whose work I could not cite due to space limitations.

Work in the author's laboratory is funded by NIH grant GM077537.

## References

1. Archibald JM. Endosymbiosis and Eukaryotic Cell Evolution. Curr Biol. 2015; 25:R911–21. DOI: 10.1016/j.cub.2015.07.055 [PubMed: 26439354]
2. Lane N, Martin W. The energetics of genome complexity. Nature. 2010; 467:929–934. DOI: 10.1038/nature09486 [PubMed: 20962839]
3. Ribbeck K, Görlich D. Kinetic analysis of translocation through nuclear pore complexes. Embo J. 2001; 20:1320–1330. DOI: 10.1093/emboj/20.6.1320 [PubMed: 11250898]
4. Galy V, Mattaj IW, Askjaer P. Caenorhabditis elegans nucleoporins Nup93 and Nup205 determine the limit of nuclear pore complex size exclusion in vivo. Mol Biol Cell. 2003; 14:5104–5115. DOI: 10.1091/mbc.E03-04-0237 [PubMed: 12937276]
5. Rout MP, Aitchison JD, Suprapto A, Hjertaas K, Zhao Y, Chait BT. The yeast nuclear pore complex: composition, architecture, and transport mechanism. J Cell Biol. 2000; 148:635–651. [PubMed: 10684247]
6. Cronshaw JM, Krutchinsky AN, Zhang W, Chait BT, Matunis MJ. Proteomic analysis of the mammalian nuclear pore complex. J Cell Biol. 2002; 158:915–927. DOI: 10.1083/jcb.200206106 [PubMed: 12196509]
7. Tamura K, Fukao Y, Iwamoto M, Haraguchi T, Hara-Nishimura I. Identification and characterization of nuclear pore complex components in Arabidopsis thaliana. Plant Cell. 2010; 22:4084–4097. DOI: 10.1105/tpc.110.079947 [PubMed: 21189294]
8. Degrasse JA, DuBois KN, Devos D, Siegel TN, Sali A, Field MC, et al. Evidence for a shared nuclear pore complex architecture that is conserved from the last common eukaryotic ancestor. Mol Cell Proteomics. 2009; 8:2119–2130. DOI: 10.1074/mcp.M900038-MCP200 [PubMed: 19525551]
9. Amlacher S, Sarges P, Flemming D, van Noort V, Kunze R, Devos DP, et al. Insight into structure and assembly of the nuclear pore complex by utilizing the genome of a eukaryotic thermophile. Cell. 2011; 146:277–289. DOI: 10.1016/j.cell.2011.06.039 [PubMed: 21784248]
10. Scheer U, Franke WW. Negative staining and adenosine triphosphatase activity of annulate lamellae of newt oocytes. J Cell Biol. 1969; 42:519–533. [PubMed: 4183078]
11. Hinshaw JE, Carragher BO, Milligan RA. Architecture and design of the nuclear pore complex. Cell. 1992; 69:1133–1141. [PubMed: 1617726]
12. Akey CW, Radermacher M. Architecture of the Xenopus nuclear pore complex revealed by three-dimensional cryo-electron microscopy. J Cell Biol. 1993; 122:1–19. [PubMed: 8314837]
13. Kiseleva E, Allen TD, Rutherford S, Bucci M, Wente SR, Goldberg MW. Yeast nuclear pore complexes have a cytoplasmic ring and internal filaments. J Struct Biol. 2004; 145:272–288. DOI: 10.1016/j.jsb.2003.11.010 [PubMed: 14960378]
14. von Appen A, Kosinski J, Sparks L, Ori A, DiGuilio AL, Vollmer B, et al. In situ structural analysis of the human nuclear pore complex. Nature. 2015; 526:140–143. DOI: 10.1038/nature15381 [PubMed: 26416747]

15. Eibauer M, Pellanda M, Turgay Y, Dubrovsky A, Wild A, Medalia O. Structure and gating of the nuclear pore complex. Nat Commun. 2015; 6:7532.doi: 10.1038/ncomms8532 [PubMed: 26112706]
16. Goldberg MW, Allen TD. The nuclear pore complex and lamina: three-dimensional structures and interactions determined by field emission in-lens scanning electron microscopy. J Mol Biol. 1996; 257:848–865. DOI: 10.1006/jmbi.1996.0206 [PubMed: 8636986]
17. Jarnik M, Aebi U. Toward a more complete 3-D structure of the nuclear pore complex. J Struct Biol. 1991; 107:291–308. [PubMed: 1725493]
18. Bui KH, von Appen A, DiGuilio AL, Ori A, Sparks L, Mackmull M-T, et al. Integrated structural analysis of the human nuclear pore complex scaffold. Cell. 2013; 155:1233–1243. DOI: 10.1016/j.cell.2013.10.055 [PubMed: 24315095]
19. Gall JG. Octagonal nuclear pores. J Cell Biol. 1967; 32:391–399. [PubMed: 10976230]
20. Neumann N, Lundin D, Poole AM. Comparative genomic evidence for a complete nuclear pore complex in the last eukaryotic common ancestor. PLoS ONE. 2010; 5:e13241.doi: 10.1371/journal.pone.0013241 [PubMed: 20949036]
21. Obado SO, Brillantes M, Uryu K, Zhang W, Ketaren NE, Chait BT, et al. Interactome Mapping Reveals the Evolutionary History of the Nuclear Pore Complex. PLoS Biol. 2016; 14:e1002365–30. DOI: 10.1371/journal.pbio.1002365 [PubMed: 26891179]
22. Brohawn SG, Partridge JR, Whittle JRR, Schwartz TU. The nuclear pore complex has entered the atomic age. Structure. 2009; 17:1156–1168. DOI: 10.1016/j.str.2009.07.014 [PubMed: 19748337]
23. Reichelt R, Holzenburg A, Buhle EL, Jarnik M, Engel A, Aebi U. Correlation between structure and mass distribution of the nuclear pore complex and of distinct pore complex components. J Cell Biol. 1990; 110:883–894. [PubMed: 2324201]
24. Alber F, Dokudovskaya S, Veenhoff LM, Zhang W, Kipper J, Devos D, et al. The molecular architecture of the nuclear pore complex. Nature. 2007; 450:695–701. DOI: 10.1038/nature06405 [PubMed: 18046406]
25. Ori A, Banterle N, Iskar M, Andrés-Pons A, Escher C, Khanh Bui H, et al. Cell type-specific nuclear pores: a case in point for context-dependent stoichiometry of molecular machines. Mol Syst Biol. 2013; 9:648–648. DOI: 10.1038/msb.2013.4 [PubMed: 23511206]
26. Schwartz TU. Modularity within the architecture of the nuclear pore complex. Curr Opin Struct Biol. 2005; 15:221–226. DOI: 10.1016/j.sbi.2005.03.003 [PubMed: 15837182]
27. Vasu S, Shah S, Orjalo A, Park M, Fischer WH, Forbes DJ. Novel vertebrate nucleoporins Nup133 and Nup160 play a role in mRNA export. J Cell Biol. 2001; 155:339–354. DOI: 10.1083/jcb.200108007 [PubMed: 11684705]
28. Siniossoglou S, Wimmer C, Rieger M, Doye V, Tekotte H, Weise C, et al. A novel complex of nucleoporins, which includes Sec13p and a Sec13p homolog, is essential for normal nuclear pores. Cell. 1996; 84:265–275. [PubMed: 8565072]
29. Finlay DR, Meier E, Bradley P, Horecka J, Forbes DJ. A complex of nuclear pore proteins required for pore function. J Cell Biol. 1991; 114:169–183. [PubMed: 2050741]
30. Grandi P, Doye V, Hurt EC. Purification of NSP1 reveals complex formation with “GLFG” nucleoporins and a novel nuclear pore protein NIC96. Embo J. 1993; 12:3061–3071. [PubMed: 7688296]
31. Fischer J, Teimer R, Amlacher S, Kunze R, Hurt E. Linker Nups connect the nuclear pore complex inner ring with the outer ring and transport channel. Nat Struct Mol Biol. 2015; 22:774–781. DOI: 10.1038/nsmb.3084 [PubMed: 26344569]
32. Stuwe T, Bley CJ, Thierbach K, Petrovic S, Schilbach S, Mayo DJ, et al. Architecture of the fungal nuclear pore inner ring complex. Science. 2015; 350:56–64. DOI: 10.1126/science.aac9176 [PubMed: 26316600]
33. Kelley K, Knockenhauer KE, Kabachinski G, Schwartz TU. Atomic structure of the Y complex of the nuclear pore. Nat Struct Mol Biol. 2015; 22:425–431. DOI: 10.1038/nsmb.2998 [PubMed: 25822992]
34. Kellner N, Schwarz J, Sturm M, Fernandez-Martinez J, Griesel S, Zhang W, et al. Developing genetic tools to exploit Chaetomium thermophilum for biochemical analyses of eukaryotic macromolecular assemblies. Sci Rep. 2016; 6:20937.doi: 10.1038/srep20937 [PubMed: 26864114]

35. Lutzmann M, Kunze R, Buerer A, Aebi U, Hurt E. Modular self-assembly of a Y-shaped multiprotein complex from seven nucleoporins. Embo J. 2002; 21:387–397. DOI: 10.1093/emboj/21.3.387 [PubMed: 11823431]
36. Rasala BA, Orjalo AV, Shen Z, Briggs S, Forbes DJ. ELYS is a dual nucleoporin/kinetochore protein required for nuclear pore assembly and proper cell division. Proc Natl Acad Sci USA. 2006; 103:17801–17806. DOI: 10.1073/pnas.0608484103 [PubMed: 17098863]
37. Loïodice I, Alves A, Rabut G, Van Overbeek M, Ellenberg J, Sibarita J-B, et al. The entire Nup107–160 complex, including three new members, is targeted as one entity to kinetochores in mitosis. Mol Biol Cell. 2004; 15:3333–3344. DOI: 10.1091/mbc.E03-12-0878 [PubMed: 15146057]
38. Devos D, Dokudovskaya S, Alber F, Williams R, Chait BT, Sali A, et al. Components of coated vesicles and nuclear pore complexes share a common molecular architecture. PLoS Biol. 2004; 2:e380.doi: 10.1371/journal.pbio.0020380 [PubMed: 15523559]
39. Devos D, Dokudovskaya S, Williams R, Alber F, Eswar N, Chait BT, et al. Simple fold composition and modular architecture of the nuclear pore complex. Proc Natl Acad Sci USA. 2006; 103:2172–2177. DOI: 10.1073/pnas.0506345103 [PubMed: 16461911]
40. Brohawn SG, Leksa NC, Spear ED, Rajashankar KR, Schwartz TU. Structural evidence for common ancestry of the nuclear pore complex and vesicle coats. Science. 2008; 322:1369–1373. DOI: 10.1126/science.1165886 [PubMed: 18974315]
41. Harel A, Orjalo AV, Vincent T, Lachish-Zalait A, Vasu S, Shah S, et al. Removal of a single pore subcomplex results in vertebrate nuclei devoid of nuclear pores. Mol Cell. 2003; 11:853–864. [PubMed: 12718872]
42. Walther TC, Alves A, Pickersgill H, Loïodice I, Hetzer M, Galy V, et al. The conserved Nup107–160 complex is critical for nuclear pore complex assembly. Cell. 2003; 113:195–206. [PubMed: 12705868]
43. Vollmer B, Antonin W. The diverse roles of the Nup93/Nic96 complex proteins - structural scaffolds of the nuclear pore complex with additional cellular functions. Biol Chem. 2014; 395:515–528. DOI: 10.1515/hsz-2013-0285 [PubMed: 24572986]
44. Schrader N, Stelter P, Flemming D, Kunze R, Hurt E, Vetter IR. Structural basis of the nic96 subcomplex organization in the nuclear pore channel. Mol Cell. 2008; 29:46–55. DOI: 10.1016/j.molcel.2007.10.022 [PubMed: 18206968]
45. Chug H, Trakhanov S, Hülsmann BB, Pleiner T, Görlich D. Crystal structure of the metazoan Nup62•Nup58•Nup54 nucleoporin complex. Science. 2015; 350:106–110. DOI: 10.1126/science.aac7420 [PubMed: 26292704]
46. Grandi P, Schlaich N, Tekotte H, Hurt EC. Functional interaction of Nic96p with a core nucleoporin complex consisting of Nsp1p, Nup49p and a novel protein Nup57p. Embo J. 1995; 14:76–87. [PubMed: 7828598]
47. Grandi P, Emig S, Weise C, Hucho F, Pohl T, Hurt EC. A novel nuclear pore protein Nup82p which specifically binds to a fraction of Nsp1p. J Cell Biol. 1995; 130:1263–1273. [PubMed: 7559750]
48. Belgareh N, Snay-Hodge C, Pasteau F, Dagher S, Cole CN, Doye V. Functional characterization of a Nup159p-containing nuclear pore subcomplex. Mol Biol Cell. 1998; 9:3475–3492. [PubMed: 9843582]
49. Stelter P, Kunze R, Flemming D, Höpfner D, Diepholz M, Philippsen P, et al. Molecular basis for the functional interaction of dynein light chain with the nuclear-pore complex. Nat Cell Biol. 2007; 9:788–796. DOI: 10.1038/ncb1604 [PubMed: 17546040]
50. Stuwe T, Schada von Borzyskowski L, Davenport AM, Hoelz A. Molecular basis for the anchoring of proto-oncoprotein nup98 to the cytoplasmic face of the nuclear pore complex. J Mol Biol. 2012; 419:330–346. DOI: 10.1016/j.jmb.2012.03.024 [PubMed: 22480613]
51. Berke IC, Boehmer T, Blobel G, Schwartz TU. Structural and functional analysis of Nup133 domains reveals modular building blocks of the nuclear pore complex. J Cell Biol. 2004; 167:591–597. DOI: 10.1083/jcb.200408109 [PubMed: 15557116]
52. Mans BJ, Anantharaman V, Aravind L, Koonin EV. Comparative genomics, evolution and origins of the nuclear envelope and nuclear pore complex. Cell Cycle. 2004; 3:1612–1637. [PubMed: 15611647]

53. Fath S, Mancias JD, Bi X, Goldberg J. Structure and organization of coat proteins in the COPII cage. Cell. 2007; 129:1325–1336. DOI: 10.1016/j.cell.2007.05.036 [PubMed: 17604721]
54. Bilokapic S, Schwartz TU. Molecular basis for Nup37 and ELY5/ELYS recruitment to the nuclear pore complex. Proc Natl Acad Sci USA. 2012; 109:15241–15246. DOI: 10.1073/pnas.1205151109 [PubMed: 22955883]
55. Xu C, Li Z, He H, Wernimont A, Li Y, Loppnau P, et al. Crystal structure of human nuclear pore complex component NUP43. FEBS Lett. 2015; 589:3247–3253. DOI: 10.1016/j.febslet.2015.09.008 [PubMed: 26391640]
56. Leksa NC, Brohawn SG, Schwartz TU. The structure of the scaffold nucleoporin Nup120 reveals a new and unexpected domain architecture. Structure. 2009; 17:1082–1091. DOI: 10.1016/j.str.2009.06.003 [PubMed: 19576787]
57. Whittle JRR, Schwartz TU. Architectural nucleoporins Nup157/170 and Nup133 are structurally related and descend from a second ancestral element. J Biol Chem. 2009; 284:28442–28452. DOI: 10.1074/jbc.M109.023580 [PubMed: 19674973]
58. Whittle JRR, Schwartz TU. Structure of the Sec13-Sec16 edge element, a template for assembly of the COPII vesicle coat. J Cell Biol. 2010; 190:347–361. DOI: 10.1083/jcb.201003092 [PubMed: 20696705]
59. Bar-Peled L, Chantranupong L, Cherniack AD, Chen WW, Ottina KA, Grabiner BC, et al. A Tumor suppressor complex with GAP activity for the Rag GTPases that signal amino acid sufficiency to mTORC1. Science. 2013; 340:1100–1106. DOI: 10.1126/science.1232044 [PubMed: 23723238]
60. Dokudovskaya S, Rout MP. SEA you later alli-GATOR - a dynamic regulator of the TORC1 stress response pathway. J Cell Sci. 2015; 128:2219–2228. DOI: 10.1242/jcs.168922 [PubMed: 25934700]
61. Kobe B, Kajava AV. When protein folding is simplified to protein coiling: the continuum of solenoid protein structures. Trends Biochem Sci. 2000; 25:509–515. [PubMed: 11050437]
62. Söding J. Protein homology detection by HMM-HMM comparison. Bioinformatics. 2005; 21:951–960. DOI: 10.1093/bioinformatics/bti125 [PubMed: 15531603]
63. Seo H-S, Ma Y, Debler EW, Wacker D, Kutik S, Blobel G, et al. Structural and functional analysis of Nup120 suggests ring formation of the Nup84 complex. Proc Natl Acad Sci USA. 2009; 106:14281–14286. DOI: 10.1073/pnas.0907453106 [PubMed: 19706512]
64. Liu X, Liu X, Mitchell JM, Wozniak RW, Blobel G, Fan J, et al. Structural evolution of the membrane-coating module of the nuclear pore complex. Proc Natl Acad Sci USA. 2012; 109:16498–16503. DOI: 10.1073/pnas.1214557109 [PubMed: 23019579]
65. Kim SJ, Fernandez-Martinez J, Sampathkumar P, Martel A, Matsui T, Tsuruta H, et al. Integrative structure-function mapping of the nucleoporin Nup133 suggests a conserved mechanism for membrane anchoring of the nuclear pore complex. Mol Cell Proteomics. 2014; 13:2911–2926. DOI: 10.1074/mcp.M114.040915 [PubMed: 25139911]
66. Stuwe T, Correia AR, Lin DH, Paduch M, Lu VT, Kossiakoff AA, et al. Nuclear pores. Architecture of the nuclear pore complex coat. Science. 2015; 347:1148–1152. DOI: 10.1126/science.aaa4136 [PubMed: 25745173]
67. Shi Y, Fernandez-Martinez J, Tjioe E, Pellarin R, Kim SJ, Williams R, et al. Structural characterization by cross-linking reveals the detailed architecture of a coatomer-related heptameric module from the nuclear pore complex. Mol Cell Proteomics. 2014; 13:2927–2943. DOI: 10.1074/mcp.M114.041673 [PubMed: 25161197]
68. Kellis M, Birren BW, Lander ES. Proof and evolutionary analysis of ancient genome duplication in the yeast Saccharomyces cerevisiae. Nature. 2004; 428:617–624. DOI: 10.1038/nature02424 [PubMed: 15004568]
69. Handa N, Kukimoto-Niino M, Akasaka R, Kishishita S, Murayama K, Terada T, et al. The crystal structure of mouse Nup35 reveals atypical RNP motifs and novel homodimerization of the RRM domain. J Mol Biol. 2006; 363:114–124. DOI: 10.1016/j.jmb.2006.07.089 [PubMed: 16962612]
70. Jeudy S, Schwartz TU. Crystal structure of nucleoporin Nic96 reveals a novel, intricate helical domain architecture. J Biol Chem. 2007; 282:34904–34912. DOI: 10.1074/jbc.M705479200 [PubMed: 17897938]

71. Seo H-S, Blus BJ, Jankovic NZ, Blobel G. Structure and nucleic acid binding activity of the nucleoporin Nup157. Proc Natl Acad Sci USA. 2013; 110:16450–16455. DOI: 10.1073/pnas.1316607110 [PubMed: 24062435]
72. Koumandou VL, Wickstead B, Ginger ML, van der Giezen M, Dacks JB, Field MC. Molecular paleontology and complexity in the last eukaryotic common ancestor. Crit Rev Biochem Mol Biol. 2013; 48:373–396. DOI: 10.3109/10409238.2013.821444 [PubMed: 23895660]
73. Flemming D, Devos DP, Schwarz J, Amlacher S, Lutzmann M, Hurt E. Analysis of the yeast nucleoporin Nup188 reveals a conserved S-like structure with similarity to karyopherins. J Struct Biol. 2012; 177:99–105. DOI: 10.1016/j.jsb.2011.11.008 [PubMed: 22138091]
74. Andersen KR, Onischenko E, Tang JH, Kumar P, Chen JZ, Ulrich A, et al. Scaffold nucleoporins Nup188 and Nup192 share structural and functional properties with nuclear transport receptors. eLife. 2013; 2doi: 10.7554/eLife.00745
75. Sampathkumar P, Kim SJ, Upla P, Rice WJ, Phillips J, Timney BL, et al. Structure, dynamics, evolution, and function of a major scaffold component in the nuclear pore complex. Structure. 2013; 21:560–571. DOI: 10.1016/j.str.2013.02.005 [PubMed: 23499021]
76. Stuwe T, Lin DH, Collins LN, Hurt E, Hoelz A. Evidence for an evolutionary relationship between the large adaptor nucleoporin Nup192 and karyopherins. Proc Natl Acad Sci USA. 2014; 111:2530–2535. DOI: 10.1073/pnas.1311081111 [PubMed: 24505056]
77. Cook A, Bono F, Jinek M, Conti E. Structural biology of nucleocytoplasmic transport. Annu Rev Biochem. 2007; 76:647–671. DOI: 10.1146/annurev.biochem.76.052705.161529 [PubMed: 17506639]
78. Süel KE, Cansizoglu AE, Chook YM. Atomic resolution structures in nuclear transport. Methods. 2006; 39:342–355. DOI: 10.1016/j.ymeth.2006.06.015 [PubMed: 16938467]
79. Pumroy RA, Cingolani G. Diversification of importin-α isoforms in cellular trafficking and disease states. Biochem J. 2015; 466:13–28. DOI: 10.1042/BJ20141186 [PubMed: 25656054]
80. Stewart M. Molecular mechanism of the nuclear protein import cycle. Nat Rev Mol Cell Biol. 2007; 8:195–208. DOI: 10.1038/nrm2114 [PubMed: 17287812]
81. Theerthagiri G, Eisenhardt N, Schwarz H, Antonin W. The nucleoporin Nup188 controls passage of membrane proteins across the nuclear pore complex. J Cell Biol. 2010; 189:1129–1142. DOI: 10.1083/jcb.200912045 [PubMed: 20566687]
82. Teixeira MT, Siniossoglou S, Podtelejnikov S, Bénichou JC, Mann M, Dujon B, et al. Two functionally distinct domains generated by in vivo cleavage of Nup145p: a novel biogenesis pathway for nucleoporins. Embo J. 1997; 16:5086–5097. DOI: 10.1093/emboj/16.16.5086 [PubMed: 9305650]
83. Gaik M, Flemming D, von Appen A, Kastritis P, Mücke N, Fischer J, et al. Structural basis for assembly and function of the Nup82 complex in the nuclear pore scaffold. J Cell Biol. 2015; 208:283–297. DOI: 10.1083/jcb.201411003 [PubMed: 25646085]
84. Romes EM, Tripathy A, Slep KC. Structure of a yeast Dyn2-Nup159 complex and molecular basis for dynein light chain-nuclear pore interaction. J Biol Chem. 2012; 287:15862–15873. DOI: 10.1074/jbc.M111.336172 [PubMed: 22411995]
85. Yoshida K, Seo H-S, Debler EW, Blobel G, Hoelz A. Structural and functional analysis of an essential nucleoporin heterotrimer on the cytoplasmic face of the nuclear pore complex. Proc Natl Acad Sci USA. 2011; 108:16571–16576. DOI: 10.1073/pnas.1112846108 [PubMed: 21930948]
86. Ren Y, Seo H-S, Blobel G, Hoelz A. Structural and functional analysis of the interaction between the nucleoporin Nup98 and the mRNA export factor Rae1. Proc Natl Acad Sci USA. 2010; 107:10406–10411. DOI: 10.1073/pnas.1005389107 [PubMed: 20498086]
87. Montpetit B, Thomsen ND, Helmke KJ, Seeliger MA, Berger JM, Weis K. A conserved mechanism of DEAD-box ATPase activation by nucleoporins and InsP6 in mRNA export. Nature. 2011; 472:238–242. DOI: 10.1038/nature09862 [PubMed: 21441902]
88. Strahm Y, Fahrenkrog B, Zenklusen D, Rychner E, Kantor J, Rosbach M, et al. The RNA export factor Gle1p is located on the cytoplasmic fibrils of the NPC and physically interacts with the FG-nucleoporin Rip1p, the DEAD-box protein Rat8p/Dbp5p and a new protein Ymr 255p. Embo J. 1999; 18:5761–5777. DOI: 10.1093/emboj/18.20.5761 [PubMed: 10610322]

89. Yokoyama N, Hayashi N, Seki T, Panté N, Ohba T, Nishii K, et al. A giant nucleopore protein that binds Ran/TC4. Nature. 1995; 376:184–188. DOI: 10.1038/376184a0 [PubMed: 7603572]

90. Wu J, Matunis MJ, Kraemer D, Blobel G, Coutavas E. Nup358, a cytoplasmically exposed nucleoporin with peptide repeats, Ran-GTP binding sites, zinc fingers, a cyclophilin A homologous domain, and a leucine-rich region. J Biol Chem. 1995; 270:14209–14213. [PubMed: 7775481]

91. Vetter IR, Nowak C, Nishimoto T, Kuhlmann J, Wittinghofer A. Structure of a Ran-binding domain complexed with Ran bound to a GTP analogue: implications for nuclear transport. Nature. 1999; 398:39–46. DOI: 10.1038/17969 [PubMed: 10078529]

92. Schrader N, Koerner C, Koessmeier K, Bangert J-A, Wittinghofer A, Stoll R, et al. The crystal structure of the Ran-Nup153ZnF2 complex: a general Ran docking site at the nuclear pore complex. Structure/Folding and Design. 2008; 16:1116–1125. DOI: 10.1016/j.str.2008.03.014 [PubMed: 18611384]

93. Partridge JR, Schwartz TU. Crystallographic and biochemical analysis of the Ran-binding zinc finger domain. J Mol Biol. 2009; 391:375–389. DOI: 10.1016/j.jmb.2009.06.011 [PubMed: 19505478]

94. Bischoff FR, Görlich D. RanBP1 is crucial for the release of RanGTP from importin beta-related nuclear transport factors. FEBS Lett. 1997; 419:249–254. [PubMed: 9428644]

95. Kutay U, Bischoff FR, Kostka S, Kraft R, Görlich D. Export of importin alpha from the nucleus is mediated by a specific nuclear transport factor. Cell. 1997; 90:1061–1071. [PubMed: 9323134]

96. Floer M, Blobel G, Rexach M. Disassembly of RanGTP-karyopherin beta complex, an intermediate in nuclear protein import. J Biol Chem. 1997; 272:19538–19546. [PubMed: 9235958]

97. Lounsbury KM, Macara IG. Ran-binding protein 1 (RanBP1) forms a ternary complex with Ran and karyopherin beta and reduces Ran GTPase-activating protein (RanGAP) inhibition by karyopherin beta. J Biol Chem. 1997; 272:551–555. [PubMed: 8995296]

98. Milo R, Jorgensen P, Moran U, Weber G, Springer M. BioNumbers--the database of key numbers in molecular and cell biology. Nucleic Acids Res. 2010; 38:D750–3. DOI: 10.1093/nar/gkp889 [PubMed: 19854939]

99. Matunis MJ, Coutavas E, Blobel G. A novel ubiquitin-like modification modulates the partitioning of the Ran-GTPase-activating protein RanGAP1 between the cytosol and the nuclear pore complex. J Cell Biol. 1996; 135:1457–1470. [PubMed: 8978815]

100. Mahajan R, Delphin C, Guan T, Gerace L, Melchior F. A small ubiquitin-related polypeptide involved in targeting RanGAP1 to nuclear pore complex protein RanBP2. Cell. 1997; 88:97–107. [PubMed: 9019411]

101. Reverter D, Lima CD. Insights into E3 ligase activity revealed by a SUMO-RanGAP1-Ubc9-Nup358 complex. Nature. 2005; 435:687–692. DOI: 10.1038/nature03588 [PubMed: 15931224]

102. Lin DH, Zimmermann S, Stuwe T, Stuwe E, Hoelz A. Structural and Functional Analysis of the C-Terminal Domain of Nup358/RanBP2. J Mol Biol. 2013; doi: 10.1016/j.jmb.2013.01.021

103. Bichel K, Price AJ, Schaller T, Towers GJ, Freund SMV, James LC. HIV-1 capsid undergoes coupled binding and isomerization by the nuclear pore protein NUP358. Retrovirology. 2013; 10:81.doi: 10.1186/1742-4690-10-81 [PubMed: 23902822]

104. Oeffinger M, Montpetit B. Emerging properties of nuclear RNP biogenesis and export. Curr Opin Cell Biol. 2015; 34:46–53. DOI: 10.1016/j.ceb.2015.04.007 [PubMed: 25938908]

105. Bonnet A, Palancade B. Regulation of mRNA trafficking by nuclear pore complexes. Genes (Basel). 2014; 5:767–791. DOI: 10.3390/genes5030767 [PubMed: 25184662]

106. Köhler A, Hurt E. Exporting RNA from the nucleus to the cytoplasm. Nat Rev Mol Cell Biol. 2007; 8:761–773. DOI: 10.1038/nrm2255 [PubMed: 17786152]

107. Mészáros N, Cibulka J, Mendiburo MJ, Romanauska A, Schneider M, Köhler A. Nuclear pore basket proteins are tethered to the nuclear envelope and can regulate membrane curvature. Dev Cell. 2015; 33:285–298. DOI: 10.1016/j.devcel.2015.02.017 [PubMed: 25942622]

108. Strambio-de-Castillia C, Blobel G, Rout MP. Proteins connecting the nuclear pore complex with the nuclear interior. J Cell Biol. 1999; 144:839–855. [PubMed: 10085285]

109. Niepel M, Molloy KR, Williams R, Farr JC, Meinema AC, Vecchietti N, et al. The nuclear basket proteins Mlp1p and Mlp2p are part of a dynamic interactome including Esc1p and the

proteasome. Mol Biol Cell. 2013; 24:3920–3938. DOI: 10.1091/mbc.E13-07-0412 [PubMed: 24152732]

110. Strambio-de-Castillia C, Niepel M, Rout MP. The nuclear pore complex: bridging nuclear transport and gene regulation. Nat Rev Mol Cell Biol. 2010; 11:490–501. DOI: 10.1038/nrm2928 [PubMed: 20571586]
111. Zimmerberg J, Kozlov MM. How proteins produce cellular membrane curvature. Nat Rev Mol Cell Biol. 2006; 7:9–19. DOI: 10.1038/nrm1784 [PubMed: 16365634]
112. Shibata Y, Hu J, Kozlov MM, Rapoport TA. Mechanisms shaping the membranes of cellular organelles. Annu Rev Cell Dev Biol. 2009; 25:329–354. DOI: 10.1146/annurev.cellbio.042308.113324 [PubMed: 19575675]
113. Antonny B. Mechanisms of membrane curvature sensing. Annu Rev Biochem. 2011; 80:101–123. DOI: 10.1146/annurev-biochem-052809-155121 [PubMed: 21438688]
114. Drin G, Casella J-F, Gautier R, Boehmer T, Schwartz TU, Antonny B. A general amphipathic alpha-helical motif for sensing membrane curvature. Nat Struct Mol Biol. 2007; 14:138–146. DOI: 10.1038/nsmb1194 [PubMed: 17220896]
115. Doucet CM, Talamas JA, Hetzer MW. Cell cycle-dependent differences in nuclear pore complex assembly in metazoa. Cell. 2010; 141:1030–1041. DOI: 10.1016/j.cell.2010.04.036 [PubMed: 20550937]
116. Marelli M, Lusk CP, Chan H, Aitchison JD, Wozniak RW. A link between the synthesis of nucleoporins and the biogenesis of the nuclear envelope. J Cell Biol. 2001; 153:709–724. [PubMed: 11352933]
117. Stavru F, Hülsmann BB, Spang A, Hartmann E, Cordes VC, Görlich D. NDC1: a crucial membrane-integral nucleoporin of metazoan nuclear pore complexes. J Cell Biol. 2006; 173:509–519. DOI: 10.1083/jcb.200601001 [PubMed: 16702233]
118. West RR, Vaisberg EV, Ding R, Nurse P, McIntosh JR. cut11(+): A gene required for cell cycle-dependent spindle pole body anchoring in the nuclear envelope and bipolar spindle formation in Schizosaccharomyces pombe. Mol Biol Cell. 1998; 9:2839–2855. [PubMed: 9763447]
119. Winey M, Hoyt MA, Chan C, Goetsch L, Botstein D, Byers B. NDC1: a nuclear periphery component required for yeast spindle pole body duplication. J Cell Biol. 1993; 122:743–751. [PubMed: 8349727]
120. Dubrovsky A, Sorrentino S, Harapin J, Sapra KT, Medalia O. Developments in cryo-electron tomography for in situ structural analysis. Arch Biochem Biophys. 2015; 581:78–85. DOI: 10.1016/j.abb.2015.04.006 [PubMed: 25921875]
121. Kühlbrandt W. Biochemistry. The resolution revolution. Science. 2014; 343:1443–1444. DOI: 10.1126/science.1251652 [PubMed: 24675944]
122. Cheng Y, Grigorieff N, Penczek PA, Walz T. A Primer to Single-Particle Cryo-Electron Microscopy. Cell. 2015; 161:438–449. DOI: 10.1016/j.cell.2015.03.050 [PubMed: 25910204]
123. Fiserova J, Kiseleva E, Goldberg MW. Nuclear envelope and nuclear pore complex structure and organization in tobacco BY-2 cells. Plant J. 2009; 59:243–255. DOI: 10.1111/j.1365-313X.2009.03865.x [PubMed: 19392704]
124. Görlich D, Kutay U. Transport between the cell nucleus and the cytoplasm. Annu Rev Cell Dev Biol. 1999; 15:607–660. DOI: 10.1146/annurev.cellbio.15.1.607 [PubMed: 10611974]
125. Weis K. Regulating access to the genome: nucleocytoplasmic transport throughout the cell cycle. Cell. 2003; 112:441–451. [PubMed: 12600309]
126. Rabut G, Doye V, Ellenberg J. Mapping the dynamic organization of the nuclear pore complex inside single living cells. Nat Cell Biol. 2004; 6:1114–1121. DOI: 10.1038/ncb1184 [PubMed: 15502822]
127. Bai X-C, McMullan G, Scheres SHW. How cryo-EM is revolutionizing structural biology. Trends Biochem Sci. 2015; 40:49–57. DOI: 10.1016/j.tibs.2014.10.005 [PubMed: 25544475]
128. Cheng Y. Single-Particle Cryo-EM at Crystallographic Resolution. Cell. 2015; 161:450–457. DOI: 10.1016/j.cell.2015.03.049 [PubMed: 25910205]

## Research Highlights

- The inventory of crystal structures of the NPC is reviewed
- The NPC is a modular assembly built from a limited set of protein domains
- Integrative approaches start to unravel the molecular NPC architecture

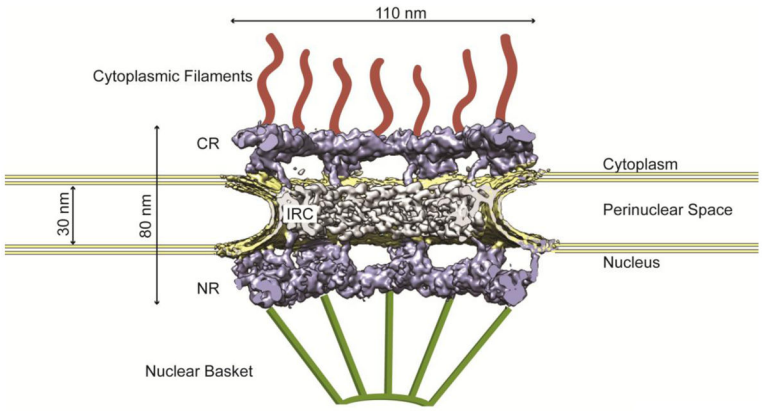


**Figure 1. Overview of the Nuclear Pore Complex**

The NPC embedded in the double membrane surrounding the nucleus of eukaryotic cells. The experimental tomographic structure EMD-3105 [14] is decorated with the nuclear basket and cytoplasmic filaments depicted schematically. CR, cytoplasmic ring; IRC, inner ring complex; NR, nucleoplasmic ring.

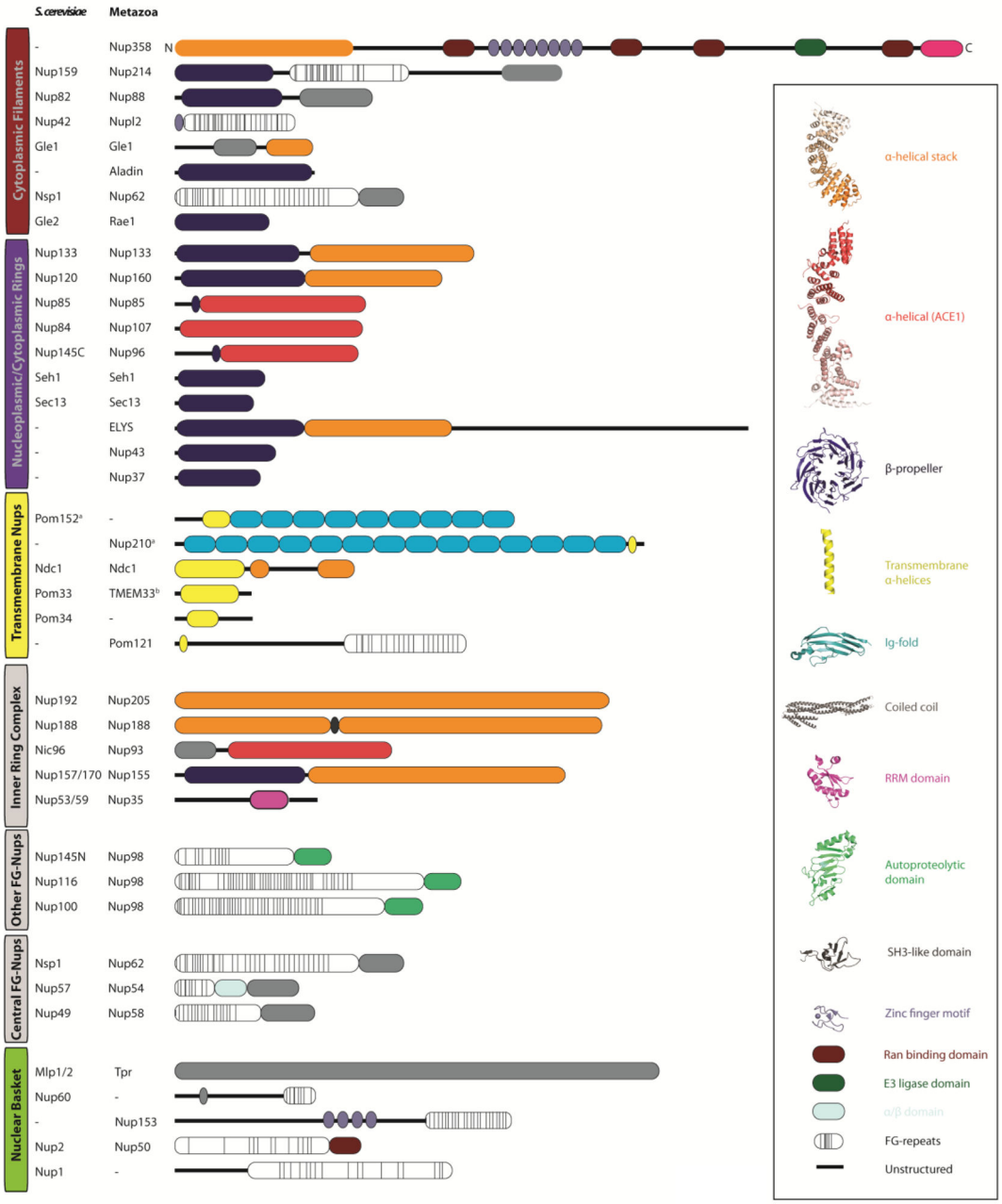


**Figure 2. Components of the Nuclear Pore Complex**

Nucleoporins making up the NPC are listed. Nomenclature for yeast (Saccharomyces cerevisiae) and metazoa, respectively, is indicated. Nucleoporins are ordered according to the subassemblies they belong to. Major domain elements are color coded and illustrated by representative crystal structures. Cartoon length approximately represents the molecular weight of each nucleoporin. The majority of nucleoporins is built up from a small set of architectural elements. Notes: [a]A chain of Immunoglobulin (Ig) folds is predicted with certainty for the luminal portions of scPom152 and hsNup210, respectively. The exact

number of Igs is unknown. [b]TMEM33 is the human homolog of scPom33, but it is not yet experimentally confirmed as a Nup.

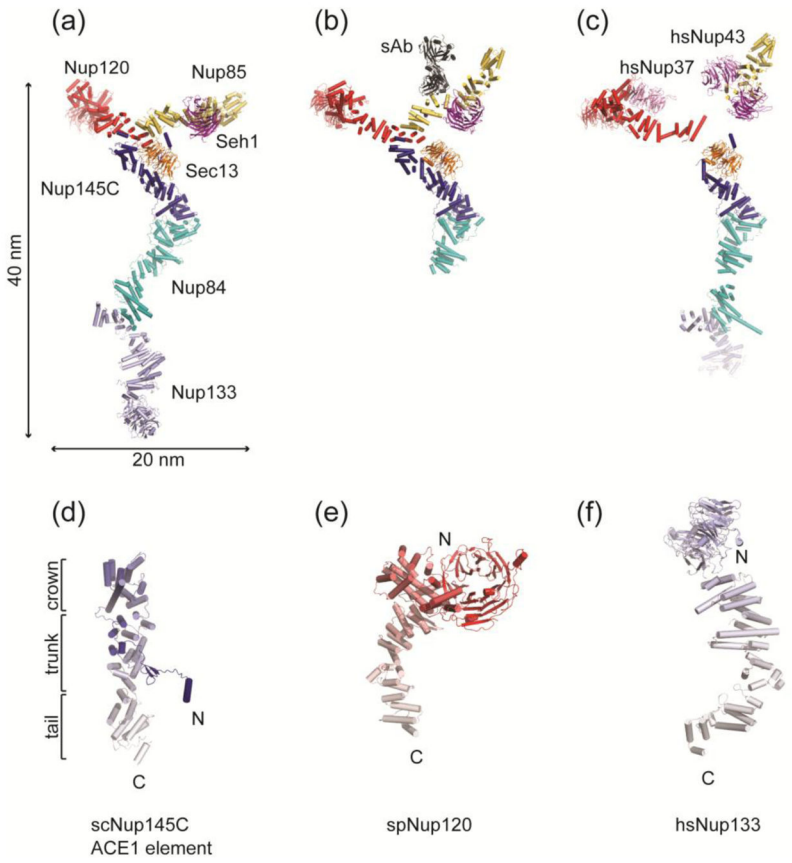


**Figure 3. Structures of Elements of the Nucleoplasmic/Cytoplasmic Rings**

The Y complex is considered to be the main building block of the NR and CR. Panels a-c show different structures of the Y complex. (a) Composite crystal structure of the complete, heptameric Y complex of *S. cerevisiae* [33]. (b) Crystal structure of a contiguous hexameric subassembly of the Y complex, with a synthetic antibody (sAb, grey) as crystallization chaperone (PDB 4XMM) [66] (c) Composite EM structure of the human Y complex, obtained by docking crystal structures into a 23 Å cryo-ET density map (PDB 5A9Q) [14]. The three assemblies are superposed using the Nup145C element as template. Differences in the position of the three extremities of the Y shaped structure can largely be explained by the intrinsic flexibility of complex. (d–f) Three differently stacked helical elements within the Y complex. scNup145C (PDB 3JRO) (d) adopts the characteristic ACE1 fold-back architecture, shared with three other scaffold nups. spNup120 (PDB 4FHN) (e) and hsNup133 (PDB 1XKS, 3I4R) (f) each combine their helical domain with an N-terminal β-propeller domain, but are otherwise structurally distinct. Color gradient to indicate the N-to-C-terminal direction.

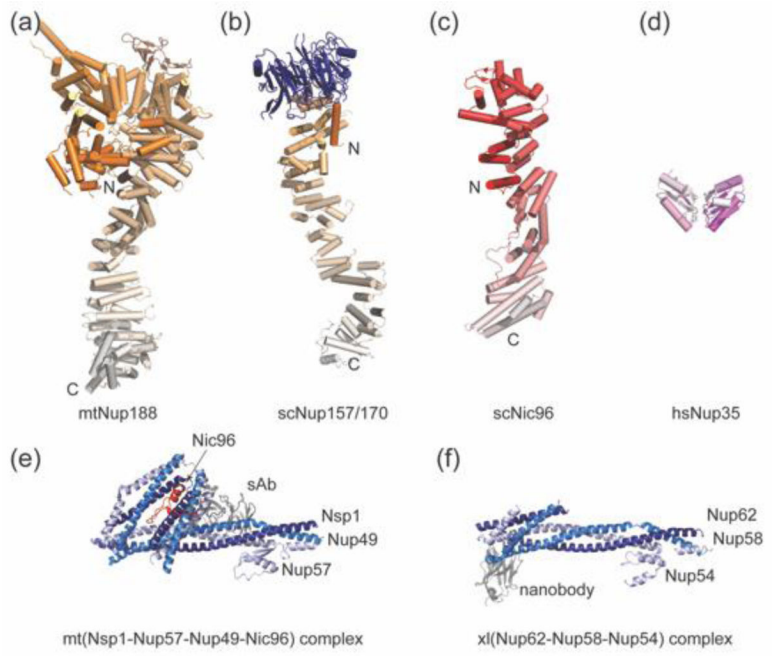


**Figure 4. Structures of Elements of the Inner Ring Complex**

The main members of the IRC have been crystallized mostly individually (a–d). (a) Composite structure of mtNup188, based on crystal structures (PDB 4KF7, 4KF8) and modeling [74]. (b) Composite structure of scNup157/170 (3I5P, 4MHC) [57,71]. (c) Crystal structure of Nic96 (PDB 2QX5, 2RFO) [70]. (d) Crystal structure of the dimerization domain of murine Nup35 (scNup53 homolog) (PDB 1WWH) [69]. (e) Crystal structure of the ct(Nsp1-Nup57-Nup49-Nic96) complex (Nic96 in red), obtained with a synthetic antibody (sAb, grey) as crystallization chaperone (PDB 5CWS) [32]. (f) Crystal structure of the metazoan Nup62-Nup58-Nup54 complex, obtained with a nanobody (grey) as crystallization chaperone (PDB 5C3L) [45]. The comparison of the Nsp1- and Nup62 complexes shows the remarkable conservation across the evolution of opisthokonts.

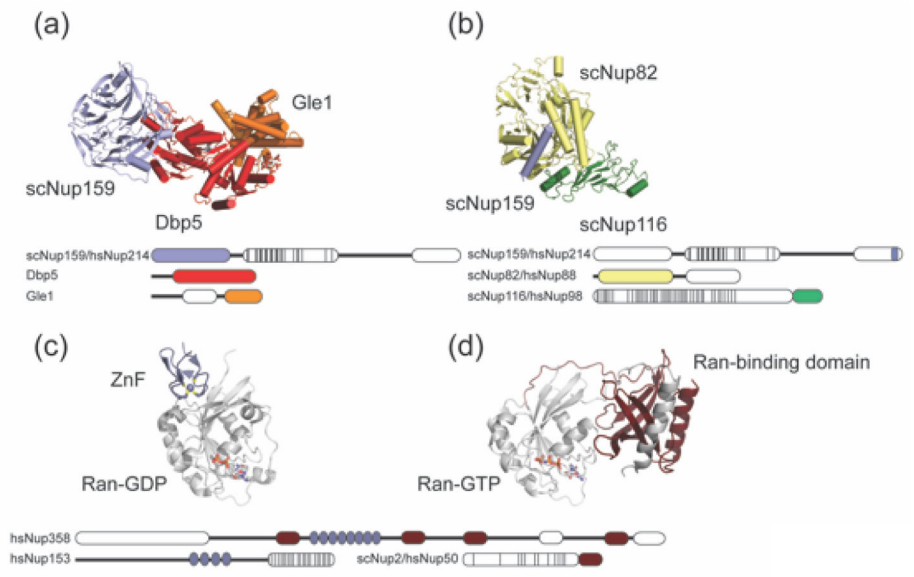


**Figure 5. Structures of Elements of the Cytoplasmic Filaments**

The structures represented in panels (a) and (b) are the most complex assemblies of the CFs known so far. (a) The trimeric sc(Nup159-Dbp5-Gle1) complex (PDB 3RRM) is an important regulatory element for mRNA export [87]. (b) The sc(Nup159-Nup82-Nup116) complex (PDB 3PBP) likely represents the anchoring element for the CF to the main NPC scaffold [85], because of the additional contacts scNup116 and its paralogs scNup100 and scNup145N can form with other nups [31,32,50]. (c, d) Ran interacts at the NPC periphery, including CF and basket and predominantly in metazoa, with elements that recognize either Ran-GDP (PDB 3GJ3–8, 3CH5) or Ran-GTP (PDB 1RRP) [91–93]. All images are paired with a schematic representation of the interacting protein fragments, color-coded to match the cartoons.